

Transfer Learning in Visual and Relational Reasoning

T.S. Jayram Vincent Marois Tomasz Kornuta Vincent Albouy
Emre Sevgen
Ahmet Ozcan
IBM Research AI
Almaden Research Center, San Jose, CA 95120, USA
Thomas J. Watson Research Center, Yorktown Heights, NY 10598, USA
{jayram, asozcan}@us.ibm.com {tkornuta, sesevgen}@gmail.com vincent.marois@ibm.com

November 19, 2019

Abstract

Transfer learning is becoming the de facto solution for vision and text encoders in the front-end processing of machine learning solutions. Utilizing vast amounts of knowledge in pre-trained models and subsequent fine-tuning allows achieving better performance in domains where labeled data is limited. In this paper, we analyze the efficiency of transfer learning in visual reasoning by introducing a new model (SAMNet) and testing it on two datasets: COG and CLEVR. Our new model achieves state-of-the-art accuracy on COG and shows significantly better generalization capabilities compared to the baseline. We also formalize a taxonomy of transfer learning for visual reasoning around three axes: feature, temporal, and reasoning transfer. Based on extensive experimentation of transfer learning on each of the two datasets, we show the performance of the new model along each axis.

1 Introduction

In recent years, neural networks, being at the epicenter of the Deep Learning [LBH15] revolution, became the dominant solutions across many domains, from Speech Recognition [GMH13], Image Classification [KSH12], Object Detection [RDGF16], to Question Answering [WCB14] and Machine Translation [BCB14] among others. At their core, being statistical models [Rip93, WM96], neural networks rely on the assumption that training and testing samples are independent and identically distributed (*iid*); i.e. sampled from a common input space under similar data distribution characteristics. However, in many real-world scenarios, this assumption does not hold. Moreover, as modern neural models often have millions of trainable parameters, training them requires vast amounts of data, which for some domains (e.g., medical) can be very expensive and/or extremely difficult to collect. One of the widely used solutions for the above mentioned problems is Transfer Learning [PY09, WKW16], a technique which enhances model performance by transferring *information* from one domain to another.

In Computer Vision, it is now standard practice to pretrain an image encoder (such as VGG [SZ14] or ResNet [HZRS16]) on large-scale datasets (such as ImageNet [DDS⁺09]), and reuse the weights in unrelated domains and tasks, such as segmentation of cars [IS18] or Visual Question Answering (VQA) in a medical domain [KRS⁺19]. Such performance improvements are appealing, especially in cases where both the domain (natural vs. medical images) and the task (image classification vs. image segmentation vs VQA) change significantly.

Similar developments have emerged in the Natural Language Processing (NLP) community. Using shallow word embeddings, such as word2vec [MSC⁺13] or GloVe [PSM14], pretrained on large corpuses from e.g. Wikipedia or Twitter, has become a standard procedure when working with different NLP domains and tasks. Recently, there is a clear, growing trend of utilization of deep contextualized word representations such as ELMo [PNI⁺18] (based on bidirectional LSTMs [HS97]) or BERT [DCLT18] (based on the Transformer [VSP⁺17] architecture), where entire deep networks (not just the input layer) are pretrained on very large corporas. In analogy to pretrained image encoders, the NLP community has also started to create model repositories, some with dozens of pretrained models ready to be downloaded and used. HuggingFace [WDS⁺19] is one of the most notable examples.

The success of transfer learning raises several research questions, such as the characteristics which make a dataset more favorable to be used in pretraining (notably ImageNet [HAE16]), or regarding the observed performance correlation of models with different architectures between the source and target domains [KSL19]. One of the most systematic works in this area is the computational taxonomic map for task transfer learning [ZSS⁺18], which aimed at discovering the dependencies between twenty-six 2D, 2.5D, 3D, and semantic computer vision tasks.

In this work we focus on transfer learning in multi-modal tasks combining vision and language [MKK19]. More precisely, we narrow the scope to transfer learning between visual reasoning tasks that have a “nice” logical structure, e.g., [JHvdM⁺17a, YGW⁺18, SSCH18]. While models such as BERT and ResNet can be transferred efficiently in the same modality they were pretrained on, challenges arise once the modalities have been fused. For example, the CoGenT (Constrained Generalization Test) variant of the CLEVR dataset [JHvdM⁺17a] contains two sets with similar questions, but differing on combinations of object-attribute values in images (Section 5.4). In this case, training on the first variant might yield entangled feature representations that may fail reasoning tasks on the second one. In video reasoning, an additional challenge in the temporal dimension is whether a model trained on shorter video sequences will transfer over to longer ones, e.g., the Canonical and the Hard variants of the COG dataset [YGW⁺18] (Section 5.3). To address these challenges, mechanisms such as attention [BCB14] and external memory [GWD14, GWR⁺16, WCB14] which facilitate higher-level abstractions, seem more promising.

Motivated by these considerations:

1. We propose a new model, called SAMNet (Selective Attention Memory Network), which achieves state-of-the-art results on COG [YGW⁺18], a Video QA reasoning dataset.
2. We propose a taxonomy of transfer learning, inspired from [PY09], applied to the domain of visual reasoning. Articulated around 3 main axes, we illustrate it through the COG dataset, as well as the CLEVR [JHvdM⁺17a] diagnostic dataset for Image QA.
3. Subsequently, we measure the impact of transferring the whole pretrained SAMNet model in the 3 proposed transfer learning settings: feature transfer, temporal transfer and reasoning transfer. This analysis is supported by an extensive set of experiments using the COG and CLEVR datasets, as well as their variants. Several of these experiments show significant transfer learning capabilities of SAMNet.

2 Related work

Visual Question Answering (VQA) [MF14, AAL⁺15] is a challenging multimodal task that combines vision and language. Most Image Question Answering datasets and tasks focus on identifying

object attributes, counting, and reasoning about their spatial-relations. Prior work generally relied on dense visual features produced by either CNNs [XMS16, YHG⁺16] or object detection modules [DCK18], and increasingly, recent models utilize the relationships among objects to augment those features with contextual information from each object’s surroundings [TLvdH17, SRB⁺17].

Another research focus area has been multimodal fusion and attention for VQA. For multi-modal fusion, earlier methods used concatenation or element-wise multiplication between multi-modal features [ZTS⁺15, AAL⁺15]. Others proposed more sophisticated methods such as different approximated bilinear pooling methods to effectively integrate the multimodal features with second-order feature interactions [FPY⁺16, KOL⁺16]. Attention research in VQA has demonstrated that learning question-guided visual attention on image regions is the most promising approach [YHG⁺16, CWC⁺15, IYF16]. Visual reasoning tasks such as the CLEVR dataset, also benefit from multi-hop attention and reasoning methods [HM18, SSCH18]. Visualization of attention maps also provides interpretability, which is an increasingly important aspect. The MAC model [HM18] is a great example of such an approach. The follow-on model by the same authors [HM19], called Neural State Machine (NSM) takes a slightly different approach and reason over graph structures rather than directly over spatial maps of visual features. Representing objects in a scene and their relationship as a graph is an obvious choice, which is another growing research direction [HRS19, TLvdH17, KYK⁺18].

Video question answering, aside from spatial queries, also focuses on questions that require *temporal* reasoning. Early works [MHSJH17, XZX⁺17, YKCK17] used LSTMs to encode video frames and text queries to leverage temporal attention to selectively attend to essential frames in a video. These approaches might be sufficient for action-recognition type of tasks but fall short when spatio-temporal reasoning is required. Learning long-term dependencies is also another challenge that LSTMs may struggle with. Yin et al. [YTXW19] recently proposed a Memory-Augmented Neural Network (MANN) architecture for video QA which leverages the external memory for storing and retrieving useful information in questions and videos and modeling long-term visual-textual dependencies.

Our work is mostly related to the MAC [HM18] as well as neural networks with external memory [GWD14, GWR⁺16] that support flexible addressing mechanisms including sequential and content-based addressing. An important distinction of our approach is the frame-by-frame processing of the video input. Prior studies typically divide the whole video into clips; e.g., in [SSCH18], the model extracts visual features from each frame and aggregates features first into clips, followed by aggregation over clips to form a single video representation. Nevertheless, when reasoning and producing the answer, the system has *access to all frames*. Similarly, in Visual Dialog [DKG⁺17], the system memorizes the whole dialog history. However, in real-time dialog or video monitoring, it is not always possible to keep the entire history of conversation nor all frames from the beginning of the recording.

3 Transfer Learning

We follow the notations in the survey by [PY09]. A *domain* is a pair $\mathcal{D} = (\mathcal{X}, P(X))$, where \mathcal{X} is a feature space and $P(X)$ is a marginal probability distribution. For visual reasoning problems considered in this paper, \mathcal{X} will consist of purely visual inputs, i.e., either images or videos in some cases, or a combination of both visual inputs and questions in other cases. A *task* is a pair $\mathcal{T} = (\mathcal{Y}, f(\cdot))$, where \mathcal{Y} is a label space and $f : \mathcal{X} \rightarrow \mathcal{Y}$ is a prediction function. When the domain elements consist of both the question and the visual input, there is only one task, namely, to answer

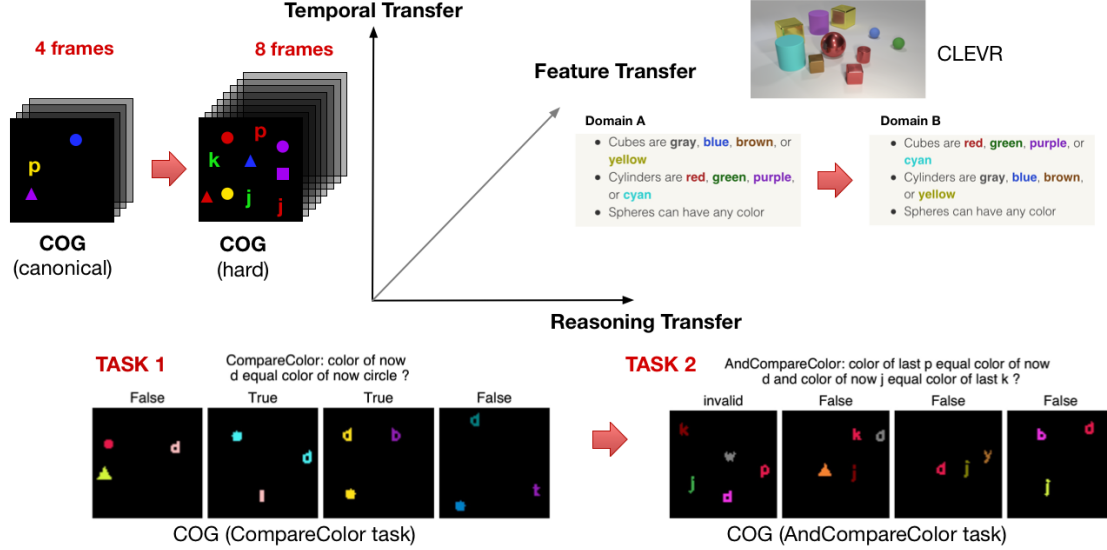


Figure 1: Transfer learning taxonomy.

the question¹. If the domain elements consist of just the visual inputs, then the task is defined by the question so that each question defines a separate task.

Definition 1 ([PY09]). *Given a source domain \mathcal{D}_S and a source learning task \mathcal{T}_S , a target domain \mathcal{D}_T and a target learning task \mathcal{T}_T , transfer learning aims to help improve the learning of the target predictive function $f_T(\cdot)$ in \mathcal{D}_T using the knowledge in \mathcal{D}_S and \mathcal{T}_S , where $\mathcal{D}_S \neq \mathcal{D}_T$, or $\mathcal{T}_S \neq \mathcal{T}_T$.*

In all our applications, $\mathcal{X}_S = \mathcal{X}_T$, so $\mathcal{D}_S \neq \mathcal{D}_T$ means that the marginal distributions P_S and P_T are different. Similarly, $\mathcal{T}_S \neq \mathcal{T}_T$ means that either $Y_S \neq Y_T$ or that the associated prediction functions are different.

Although Definition 1 is quite general, it does not adequately capture all artifacts present in visual reasoning. For example, consider the transfer learning setting where the tasks \mathcal{T}_S and \mathcal{T}_T are the same but the marginal distributions P_S and P_T are different (referred to as *domain adaptation*). As mentioned in the introduction, one setting is the case of static images, where this could be due to having different feature combinations in the source and target. A different setting is in the context of video reasoning where the number of frames can increase significantly going from source to target. These require possibly very different methods: the first involves building disentangled feature representations that can generalize across domains; the second might need external memory to remember relevant objects to generalize across frame lengths. Another situation is when the questions themselves can be grouped into families such as count-based queries, comparison of objects, or existence of objects with certain features etc. This entails studying transfer learning between families of tasks which requires extending the above definition.

Broadly, we consider 3 kinds of transfer learning problems in this work, as illustrated in Figure 1. Let \mathcal{Q} denote the set of questions and \mathcal{V} denote the set of visual inputs.

Feature Transfer: In this setting of domain adaptation, $\mathcal{X}_S = \mathcal{X}_T \subseteq \mathcal{Q} \times \mathcal{V}$ and the task $f(q, v)$ is just the answer to the question q on visual input v . The output set \mathcal{Y} is the union of legitimate answers over all questions in \mathcal{Q} . The marginal distributions P_S and P_T differ in the feature attributes such as shape, color, and size, or their combinations thereof.

¹For the COG dataset, the answer is a tuple, one for each frame in the video, whereas for typical video answering datasets, only a single answer is needed for the entire video.

Temporal Transfer: This setting is similar to attribute adaptation in that $\mathcal{X}_S = \mathcal{X}_T \subseteq \mathcal{Q} \times \mathcal{V}$ and there is a single task. The key difference is that we introduce a notion of complexity $C(v) = (n, m)$ for a visual input v , where n equals the maximum number of objects n in an image, and m equals the number of frames in a video. For any visual input v_S coming from \mathcal{X}_S with $C(v_S) = (n_S, m_S)$ and for any visual input v_T coming from \mathcal{X}_T with $C(v_T) = (n_T, m_T)$, we require that $n_T \geq n_S$ and $m_T \geq m_S$ with at least one inequality being a strict one. Thus, we necessarily increase the complexity of the visual input going from the source to the target domain.

Reasoning Transfer: This setting requires an extension of Definition 1 above to investigate transfer learning when grouping questions into families. Let \mathcal{V} be the feature space consisting of visual inputs only, shared by all tasks, with a common marginal distribution $P(X)$. For each question $q \in \mathcal{Q}$, we define the task $\mathcal{T}_q = (\mathcal{Y}_q, f_q(\cdot))$ where the output set \mathcal{Y}_q is the set of legitimate answers to q and $f_q(v)$, for a visual input v , is the answer to question q on visual input v . Thus, tasks are in a 1-1 correspondence with questions. A *task family* is a probability distribution on tasks which in our case can be obtained by defining the distribution on \mathcal{Q} . Given a task family, the goal is to learn a prediction function that gives an answer to $f_q(v)$ for $v \in \mathcal{V}$ chosen according to the feature space distribution and q chosen according to the task probability distribution. Suppose \mathcal{F}_S is the source task family and \mathcal{F}_T is the target task family. Transfer learning aims to help improve the learning of the predictive function for the target task family using the knowledge in the source task family.

If labeled data is available for \mathcal{X}_T , a training algorithm distinction we make is between *zero-shot learning* and *finetuning*. Finetuning entails the use of labeled data in the target domain \mathcal{D}_T , foreseeing performance gain on the target task \mathcal{X}_T , after initial training on \mathcal{X}_S and additional training on \mathcal{X}_T . Zero-shot learning thus refers to immediate test on \mathcal{X}_T after initial training on \mathcal{X}_S .

4 Selective Attention Memory (SAM) Network

SAM Network (SAMNet for short) is an end-to-end differentiable recurrent model equipped with an external memory (Figure 2). At the conceptual level, SAMNet draws from two core ideas: iterative reasoning as proposed e.g. in MAC (Memory-Attention-Composition) Network [HM18, MJA⁺18] and use of an external memory, as in Memory-Augmented Neural Networks such as NTM (Neural Turing Machine) [GWD14], DNC (Differentiable Neural Computer) [GWR⁺16] or DWM (Differentiable Working Memory) [JBM⁺18].

A distinctive feature of the SAM Network is its frame-by-frame temporal processing approach, where a single frame can be accessed at once. This is a notable difference from [HRS19], which uses graph traversal reasoning. The recurrent nature of SAMNet does not prevent frame sequences longer than those used for training. The memory locations store relevant objects representing contextual information about words in text and visual objects extracted from video. Each location of the memory stores a d -dimensional vector. The memory can be accessed through either content-based addressing, via dot-product attention, or location-based addressing. Using gating mechanisms, correct objects can be retrieved in order to perform multi-step spatio-temporal reasoning over text and video. A notable feature of this design is that the number of addresses N can be changed between training and testing, to fit the data characteristics.

SAMNet’s core is a recurrent cell called the SAM Cell. Unrolling a new series of T cells for each frame allows T steps of iterative reasoning, similar to [HM18]. Information flows between frames through the external memory. During the t -th reasoning step, for $t = 1, 2, \dots, T$, SAM Cell

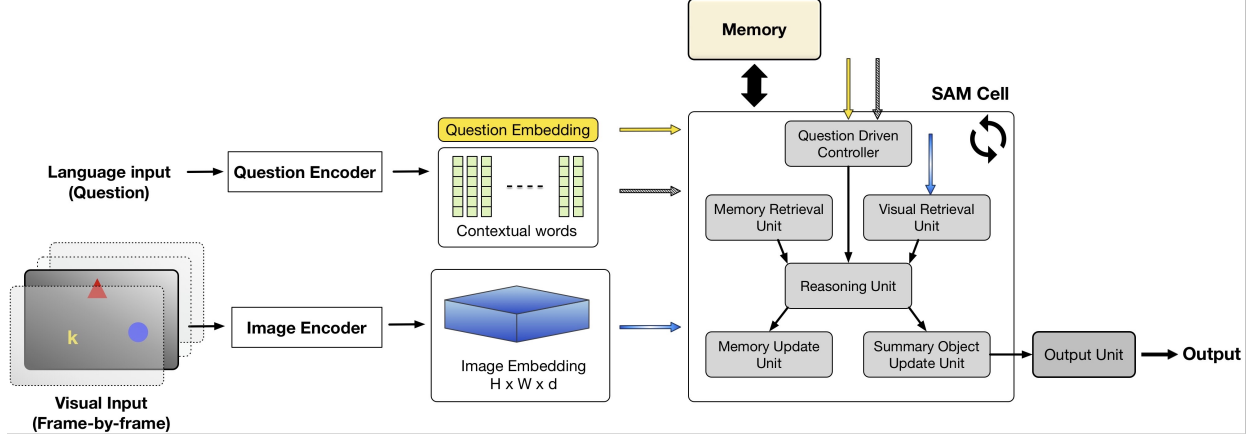


Figure 2: General architecture of SAMNet.

maintains the following information as part of its recurrent state: (a) $\mathbf{c}_t \in \mathbb{R}^d$, the control state used to drive reasoning over objects in the frame and memory; and (b) $\mathbf{so}_t \in \mathbb{R}^d$, the summary visual object representing the relevant object for step t . Let $\mathbf{M}_t \in \mathbb{R}^{N \times d}$ denote the external memory with N slots at the end of step t . Let $\mathbf{wh}_t \in \mathbb{R}^N$ denote an attention vector over the memory locations; in a trained model, \mathbf{wh}_t points to the location of the first empty slot in memory for adding new objects.

Question-driven Controller. This module drives attention over the question to produce k control states, one per reasoning operation. The control state \mathbf{c}_t at step t is then fed to a *temporal classifier*, a two-layer feedforward network with ELU activation in the hidden layer of d units. The output $\boldsymbol{\tau}_t$ of the classifier is intended to represent the different temporal contexts (or lack thereof) associated with the word in focus for that reasoning step. For the COG dataset, we pick 4 classes to capture the terms labeled “last”, “latest”, “now”, and “none”.

The visual retrieval unit uses the information generated above to extract a relevant object \mathbf{vo}_t from the frame. A similar operation on memory yields the object \mathbf{mo}_t . The memory operation is based on attention mechanism, and resembles content-based addressing. Therefore, we obtain an attention vector over memory addresses that we interpret to be the *read head*, denoted by \mathbf{rh}_t .

Reasoning Unit. This module is the backbone of SAMNet, which determines the gating operations to be performed on the external memory, as well as determining the correct object’s location for reasoning. To resolve whether we have a valid object from the frame (and similarly for memory), we execute the following reasoning procedure. First, we compute a simple aggregate² of the visual attention vector \mathbf{va}_t of dimension L (L denotes the number of feature vectors for the frame): $vs_t = \sum_{i=1}^L [\mathbf{va}_t(i)]^2$. It can be shown that the more localized the attention vector, the higher the aggregate value. We perform a similar computation on the read head \mathbf{rh}_t over memory locations. We input these two values, along with the temporal class weights $\boldsymbol{\tau}_t$, into a 3-layer feedforward classifier with hidden ELU units to extract 4 gating values (in $[0, 1]$) for the current reasoning step: (a) g_t^v , which determines whether there is a valid visual object; (b) g_t^m , which determines whether there is a valid memory object. (c) h_t^i , which determines whether the memory should be updated by replacing a previously stored object with a new one; and (d) h_t^a , which determines whether a new object should be added to memory. We stress that the network has to learn via training how to correctly implement these behaviors.

Memory Update Unit. The unit first determines the memory location where an object could

²This is closely related to Rényi entropy and Tsallis entropy of order 2.

be added:

$$\mathbf{w}_t = h^r \cdot \mathbf{r}\mathbf{h}_t + h^a \cdot \mathbf{w}\mathbf{h}_{t-1}$$

Above, \mathbf{w}_t denotes the pseudo-attention vector that represents the “location” where the memory update should happen. \mathbf{w}_t sums up to at most 1 and can be zero, indicating in this case there is no need adding a new object nor replacing an existing object. We then update the memory accordingly as:

$$\mathbf{M}_t = \mathbf{M}_{t-1} \odot (\mathbf{J} - \mathbf{w}_t \otimes \mathbf{1}) + \mathbf{w}_t \otimes \mathbf{v}\mathbf{o}_t,$$

where $\mathbf{v}\mathbf{o}_t$ denotes the object returned by the visual retrieval unit. Here \mathbf{J} denotes the all ones matrix, \odot denotes the Hadamard product and \otimes denotes the Kronecker product. Note that the memory is unchanged in the case where $\mathbf{w}_t = 0$, i.e., $\mathbf{M}_t = \mathbf{M}_{t-1}$. We finally update the write head so that it points to the succeeding address if an object was added to memory or otherwise stay the same. Let $\mathbf{w}\mathbf{h}'_{t-1}$ denote the circular shift to the right of $\mathbf{w}\mathbf{h}_{t-1}$ which corresponds to the soft version of the head update. Then:

$$\mathbf{w}\mathbf{h}_t = h^a \cdot \mathbf{w}\mathbf{h}'_{t-1} + (1 - h^a) \cdot \mathbf{w}\mathbf{h}_{t-1}$$

Summary Update Unit. This unit updates the (recurrent) summary object to equal the outcome of the t -th reasoning step. We first determine whether the relevant object $\mathbf{r}\mathbf{o}_t$ should be obtained from memory or the frame according to:

$$\mathbf{r}\mathbf{o}_t = g_t^v \cdot \mathbf{v}\mathbf{o}_t + g_t^m \cdot \mathbf{m}\mathbf{o}_t$$

Note that $\mathbf{r}\mathbf{o}_t$ is allowed to be a null object (i.e. 0 vector) in case neither of the gates evaluate to true. Finally, $\mathbf{s}\mathbf{o}_t$ is the output of a linear layer whose inputs are $\mathbf{r}\mathbf{o}_t$ and the previous summary object $\mathbf{s}\mathbf{o}_{t-1}$. This serves to retain additional information in $\mathbf{s}\mathbf{o}_{t-1}$, e.g., if it held the partial result of a complex query with Boolean connectives.

5 Experiments

We implemented and trained our SAMNet model using MI-Prometheus [KMM⁺18], a framework based on Pytorch [PGC⁺17]. We evaluated the model on the COG dataset [YGW⁺18], a video reasoning [MKK19] dataset developed for the purpose of research on relational and temporal reasoning, as well as on the CLEVR dataset [JHvdM⁺17a], created for Image Question Answering research. There are 23 classification question categories in COG and the 5 original question categories in CLEVR. Our experiments were designed to study SAMNet’s performance in terms of generalization and transfer learning abilities in different settings, and involved incorporating variants of both datasets. For COG, the Canonical (easy) and Hard variant differ mainly on the number of frames in the video, the maximum amount of look-back in frame history containing relevant information for reasoning, and the number of object distractors (see Table 1). For CLEVR, we consider the CoGenT (Constrained Generalization Test) variant which contains two conditions, differing on the combinations of attribute values (details in Section 5.3).

Variant	Frames	History	Distractors
Canonical (Easy)	4	3	1
Hard	8	7	10

Table 1: Details of the Canonical and Hard variants of COG.

5.1 Performance of SAMNet vs baseline model [YGW⁺18]

We trained SAMNet using 8 reasoning steps and external memory of 8 address locations, each storing an array of 128 floats. We compared our results with the baseline model introduced in the same paper as the COG dataset [YGW⁺18]. The most important results are highlighted in Figure 3; full comparison can be found in the supplementary material.

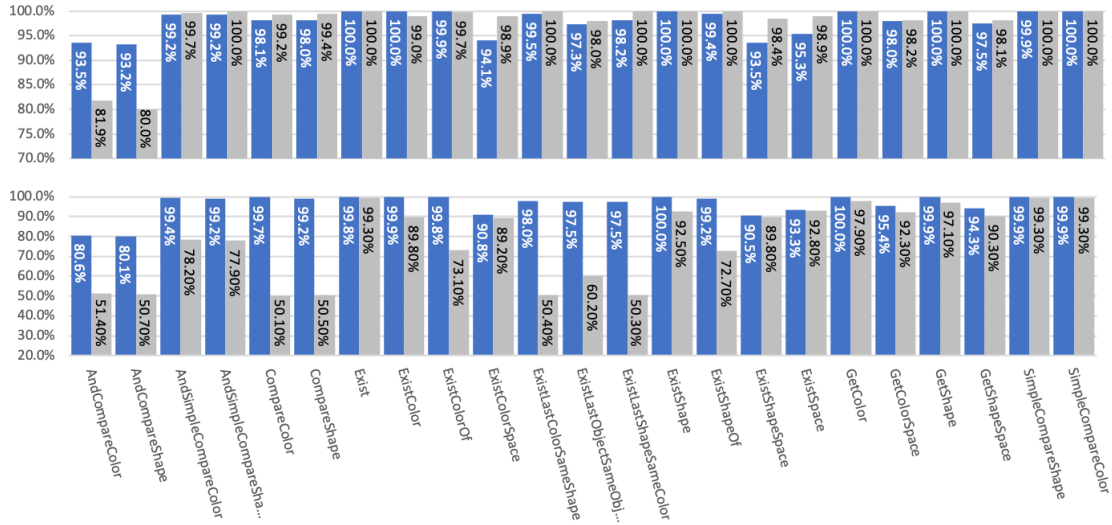


Figure 3: Comparison of test set accuracies of SAMNet (blue) with original results achieved by the baseline model [YGW⁺18] (gray) on Canonical (top) and Hard (bottom) variants of the COG dataset.

For the Canonical variant (top row), we achieve similar accuracies for the majority of tasks (with a total average accuracy of 98.0%, compared to 97.6% for the baseline model), with significant improvements (around 13 points) for *AndCompare* tasks. As these tasks focus on compositional questions referring to two objects, we hypothesize that our model achieves better accuracy due to its ability to selectively pick and store relevant objects from the past frames in memory. For the Hard variant, we achieve a total average accuracy of 96.1% compared to 80.1% for the baseline model, demonstrating that our model can adapt to larger number of frames and distractors. Despite there being some tasks in the Canonical variant where SAMNet achieved slightly lower accuracies, when comparing performances on the Hard variant, it improves upon the baseline model on all tasks, with improvements varying from 0.5 to more than 30 points, and especially on the more complex tasks in the dataset.

5.2 Reasoning transfer on CLEVR and COG

In these experiments using the CLEVR and COG datasets, we focus on analyzing the impact of each task relative to others using appropriate groupings of tasks.

5.2.1 CLEVR

For the CLEVR dataset, we consider the question categories defined by the authors: *Exist*, *Count*, *CompareInteger*, *CompareAttribute*, *QueryAttribute*. For performance reasons, we deactivated the external memory and temporally-related modules in SAMNet as they are unnecessary while reasoning about static images. We conduct the following experiments:

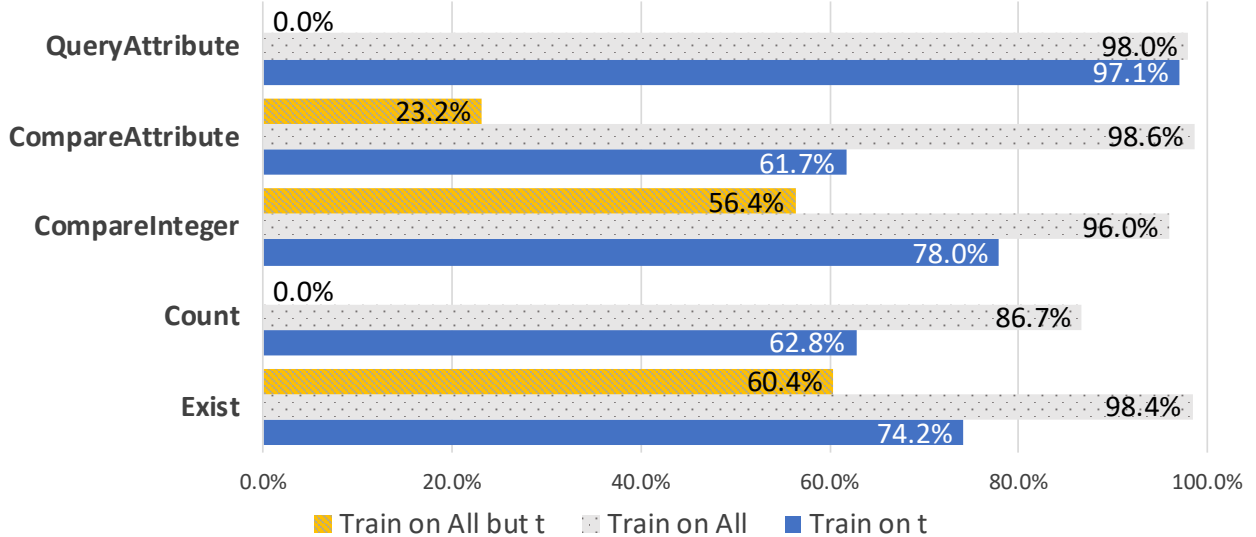


Figure 4: CLEVR-CoGenT accuracies for all tasks t when training on t only, training on all tasks jointly and training on all tasks but t .

- Train and test SAMNet on a single task group t . These 5 experiments fit into the traditional ML setup of single-task learning;
- Train SAMNet on all task groups jointly and evaluate its performance on each task group t separately. This is a transfer learning setting where for the source task family, the task is sampled from all questions, while for the target task family, the samples consist of questions from group t only;
- Finally, for each task group t , we train SAMNet on all tasks but t , and test its performance on t . This can also be viewed as a transfer learning setting similar to the previous case.

Noticeable results are shown in Figure 4, while the complete set is available in the supplementary material.

Looking at Figure 4, SAMNet does well on *Count* and *QueryAttribute*, but poorer on the 3 other tasks in the single-task learning setting (blue). Indeed, *Exist*, *CompareInteger* and *CompareAttribute* are binary tasks; *Count* has output labels digits 0 through 10 (so <10% accuracy by chance) and *QueryAttribute* maps to the set of object-attribute values (15 labels).

Nevertheless, significant accuracy gains are noted when training jointly on all tasks (gray), ranging from 18 points to 37 points on 4 out of 5 tasks. These improvements suggest that related tasks benefit from joint training. *QueryAttribute* only sees an increase of one point. One could qualify it as *self-sufficient* as it does not appear to benefit from joint training with other tasks.

Finally, the “all-tasks-but- t ” experiments (yellow) demonstrate that while tasks are related, one does not subsume another in terms of learning. Indeed, we can observe that for *CompareAttribute*, while *Exist* and *CompareInteger* share the same output space, including them and holding out *CompareAttribute* from the training set results in poor accuracy. We also observe no learning for *Count* and *QueryAttribute*. As these categories have labels that do not overlap with other categories, the model cannot predict these labels.

An additional set of experiments, for which results are available in the supplementary material, fine-tune the model trained on all tasks on each task t respectively. Fine-tuning did not demonstrate a clear benefit (except for *Count*, where the accuracy increased by 1.5 pt) without hurting performance on the other tasks. Nevertheless, these experiments leave open the possibility that joint training of tasks may potentially benefit from using weighted sampling towards the tail end

with more emphasis on samples from less performing task groups, similar to [GHH⁺18, KGC18].

5.2.2 COG

Since the number of task classes (=23) in the COG dataset is large, we designed a 2-level hierarchy of task groups using the description of these tasks, as shown in Figure 5.

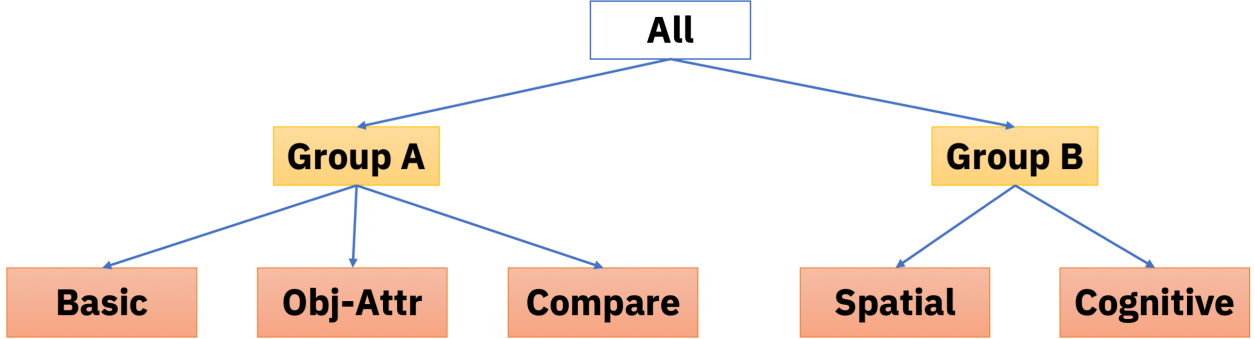


Figure 5: Hierarchy of Task Groups.

For groups at the lowest level, we chose the following task classes to be placed in those groups. Below, substitute each of *Shape* and *Color* for \underline{X} to obtain the task class.

Basic: *Exist \underline{X}* , *Get \underline{X}* and *Exist*;

Obj-Attr: *SimpleCompare \underline{X}* and *AndSimpleCompare \underline{X}* ;

Compare: *Compare \underline{X}* , *AndCompare \underline{X}* & *Exist \underline{X} Of*;

Spatial: *ExistSpace*, *Exist \underline{X} Space*, and *Get \underline{X} Space*;

Cognitive: *ExistLastColorSameShape*, *ExistLastShapeSameColor* and *ExistLastObjectSameObject*

We then conducted the following experiments using the Canonical variant of COG to study whether transfer learning was effective in leveraging information gained by training a task family at a higher level of the hierarchy:

- Train and test SAMNet on each of the 5 task groups at the lowest level of the hierarchy (Single-task training);
- Jointly train on:
 - **Group A** and test on each task from the lowest groups (i.e. **Basic**, **Obj-Attr** and **Compare**) separately;
 - **Group B** and test separately on **Spatial** and **Cognitive**;
- As a baseline, we compared the above results to the earlier experiment shown in Figure 3, which can be viewed as training jointly on **All** and testing on each group at the leaf level separately (All-task training).

The results of these experiments are shown in Figure 6.

First, notice that for each of the **Basic** and **Obj-Attr** task families, the accuracy is near-perfect in all cases, suggesting that each contains the most primitive tasks and therefore do not benefit from training with other task families. With **Spatial**, we see a small improvement showing that there is some benefit due to joint training with other task families. Two groups that demonstrated a huge improvement of more than 25 points are **Compare** and **Cognitive**. The former saw an accuracy jump from 68.6% by training on samples from that family alone to 97.0% when training

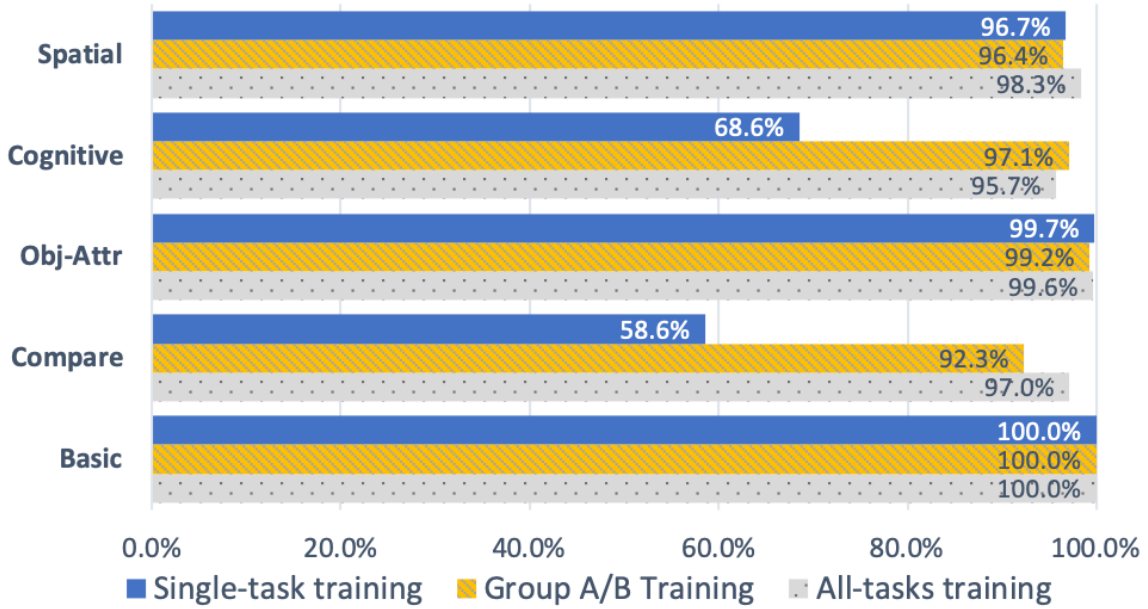


Figure 6: COG accuracies for all task groups t when training on t only; training on Group A or B; and on all tasks.

on all samples. To further emphasize this behavior, notice that just joining **Compare** with **Obj-Attr** and **Basic** already causes a significant accuracy jump to 92.3%. In hindsight, this is not surprising, as the questions in **Compare** are composed of fragments of questions given by **Basic** and **Obj-Attr**, and therefore can leverage the reasoning strategies developed there to reason about questions in **Compare**. Lastly, for the **Spatial** family, we again see the benefits of joint training with all questions (68.6% to 95.7%) but in this case there is a slight loss incurred by including everything. As seen in the figure, just jointly training with **Spatial** alone is sufficient to get a boost in accuracy (97.1%). To summarize, while joint training helps, one needs to determine how much of correlation is present with the other tasks.

5.3 Temporal transfer in COG

The goal here is to test the transfer learning ability concerning the frame sequence length, frame history required for reasoning, and the number of object distractors. For that purpose, we compare both models when trained on the Canonical variant but tested on the Hard variant (Figure 7). The light gray color indicates original accuracies of the baseline model from paper, whereas dark gray indicates accuracies of the baseline model obtained by running the original code provided by the authors [Gan18].

The first column displays the scores of the traditional ML setup when training and testing on the Canonical variant. The observed close scores in light and dark gray underscore the baseline model reproducibility. For both cases of zero-shot learning (second column–91.6% vs 65.9%) and fine-tuning using a single epoch (third column–96.7% vs. 78.1%), SAMNET outperforms the baseline model significantly. Interestingly, this fine-tuning yields a mild boost of +0.6% on the earlier reported accuracy in Section 5.1 (fourth column). These results suggest that it suffices to train SAMNet on simpler videos to enable learning of good memory usage and attention on relevant entities in order to achieve comparable, if not better, performance on longer video frames with more complex scenes.

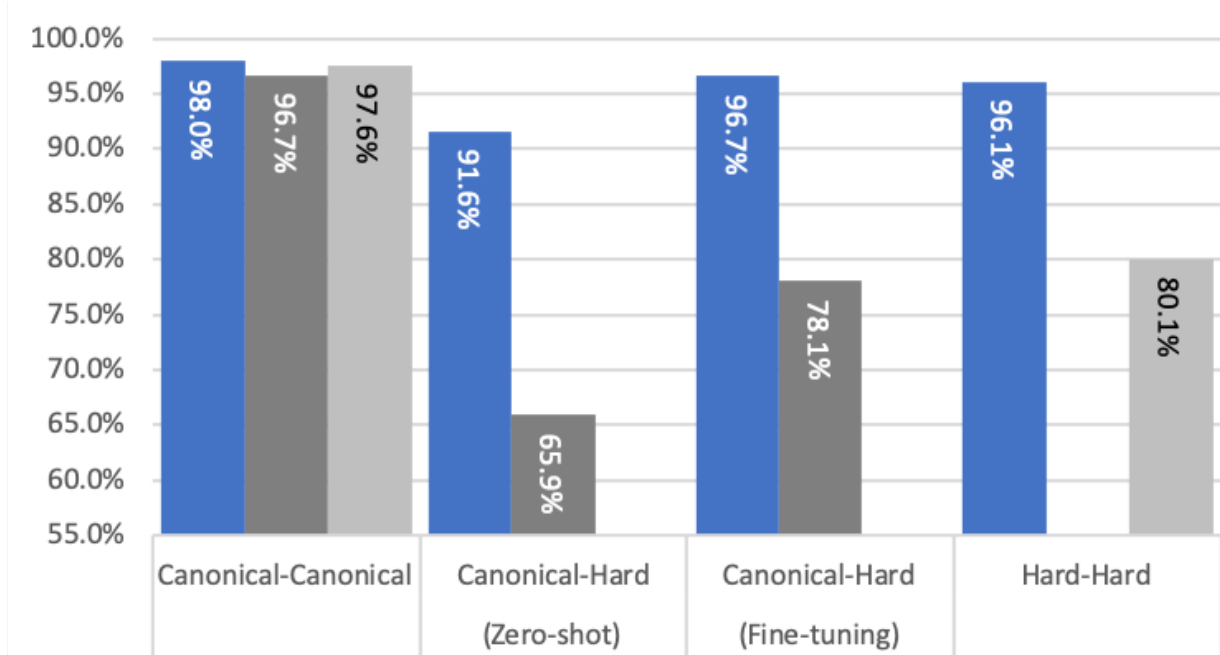


Figure 7: Total accuracies of SAMNet (blue) and baseline models (light/dark gray) when testing generalization from Canonical to Hard variants of the dataset.

5.4 Feature transfer on CLEVR-CoGenT

Dataset	Cubes	Cylinders	Spheres
CoGenT A	Family A	Family B	Any color
CoGenT B	Family B	Family A	Any color

Table 2: Restrictions on feature combinations in A & B conditions of the CoGenT variant of the CLEVR dataset.

The final set of experiments we consider is related to feature transfer. The CoGenT-A & -B variants of CLEVR differ by the available combinations of 8 object color-attributes. The colors are partitioned into two complementary families: Gray, Blue, Brown and Yellow in **Family A** and Red, Green, Purple, Cyan in **Family B**. The cubes and cylinders take colors from complementary families in each variant with opposite configurations while the spheres can take any color (See Table 2). As the input domain consist of the set of objects with all attribute values, both variants differ by their marginal distributions P_S and P_T . We conduct 2 experiments with SAMNet trained on CoGenT-A:

- an immediate test (zero-shot learning) from A to B; and
- fine-tuning for a single epoch on 30k samples from CoGenT-B (following [JHvdM⁺17b, MTSM18, PSDV⁺18, MJA⁺18]).

Performance of SAMNet on CoGenT (Figure 8) is clearly worse on CoGenT-B than CoGenT-A. Fine-tuning for a single epoch allows an observable increase of 15 pts on CoGenT-B, and a slight drop on CoGenT-A. Both are consistent with findings from the literature [JHvdM⁺17b, MTSM18, PSDV⁺18].

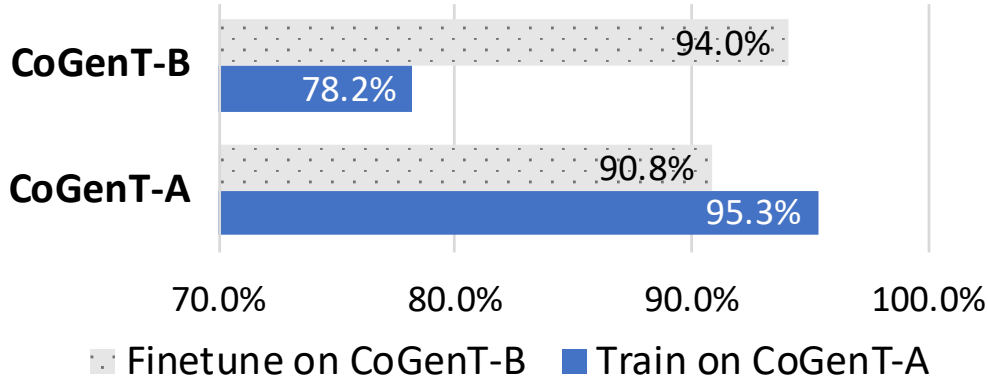


Figure 8: Test accuracy on CoGenT-A & -B when training on CoGenT-A (blue) and fine-tuning on CoGenT-B (gray).

6 Summary

In this paper, we quantified the impact of Transfer Learning on Visual Reasoning. We have proposed a new taxonomy of transfer learning for Visual Reasoning, articulated around three axes: feature, temporal and reasoning transfer. We have also introduced a novel Memory-Augmented Neural Network model called SAMNet. SAMNet, designed to learn to reason over sequences of frames, shows significant improvements over SOTA models on the COG dataset for Video Reasoning and achieves comparable performance on the CLEVR dataset for Image Reasoning.

Taking that as a starting point and leveraging the proposed taxonomy, we have conducted an extensive set of experiments, focusing on the impact of transfer learning in areas that might be considered as higher-level reasoning. SAMNet demonstrates very good generalization capabilities along certain axes and, through the cautious use of fine-tuning, can see its performance advanced even further.

Finally, we note that some of the proposed tasks (e.g. Train on all but t) are complementary to ones already well established in the literature, e.g. in Taskonomy [ZSS⁺18]. We hope these contributions will bolster new research directions to acutely apply transfer learning to areas in need of data and continue exploring the conceivable performance improvements.

References

- [AAL⁺15] Stanislaw Antol, Aishwarya Agrawal, Jiasen Lu, Margaret Mitchell, Dhruv Batra, C. Lawrence Zitnick, and Devi Parikh. VQA: Visual Question Answering. In *International Conference on Computer Vision (ICCV)*, 2015.
- [BCB14] Dzmitry Bahdanau, Kyunghyun Cho, and Yoshua Bengio. Neural machine translation by jointly learning to align and translate. *arXiv preprint arXiv:1409.0473*, 2014.
- [CWC⁺15] Kan Chen, Jiang Wang, Liang-Chieh Chen, Haoyuan Gao, Wei Xu, and Ram Nevatia. Abc-cnn: An attention based convolutional neural network for visual question answering. *arXiv preprint arXiv:1511.05960*, 2015.

- [DCK18] Mikyas T Desta, Larry Chen, and Tomasz Kornuta. Object-based reasoning in vqa. In *2018 IEEE Winter Conference on Applications of Computer Vision (WACV)*, pages 1814–1823. IEEE, 2018.
- [DCLT18] Jacob Devlin, Ming-Wei Chang, Kenton Lee, and Kristina Toutanova. Bert: Pre-training of deep bidirectional transformers for language understanding. *arXiv preprint arXiv:1810.04805*, 2018.
- [DDS⁺09] Jia Deng, Wei Dong, Richard Socher, Li-Jia Li, Kai Li, and Li Fei-Fei. Imagenet: A large-scale hierarchical image database. In *2009 IEEE conference on computer vision and pattern recognition*, pages 248–255. Ieee, 2009.
- [DKG⁺17] Abhishek Das, Satwik Kottur, Khushi Gupta, Avi Singh, Deshraj Yadav, José MF Moura, Devi Parikh, and Dhruv Batra. Visual dialog. In *Proceedings of the IEEE Conference on Computer Vision and Pattern Recognition*, pages 326–335, 2017.
- [FPY⁺16] Akira Fukui, Dong Huk Park, Daylen Yang, Anna Rohrbach, Trevor Darrell, and Marcus Rohrbach. Multimodal compact bilinear pooling for visual question answering and visual grounding. *arXiv preprint arXiv:1606.01847*, 2016.
- [Gan18] Igor Ganichev. Cog implementation. <https://github.com/google/cog>, 2018.
- [GHH⁺18] Michelle Guo, Albert Haque, De-An Huang, Serena Yeung, and Li Fei-Fei. Dynamic task prioritization for multitask learning. In *Proceedings of the European Conference on Computer Vision (ECCV)*, pages 270–287, 2018.
- [GMH13] Alex Graves, Abdel-rahman Mohamed, and Geoffrey Hinton. Speech recognition with deep recurrent neural networks. In *2013 IEEE international conference on acoustics, speech and signal processing*, pages 6645–6649. IEEE, 2013.
- [GWD14] Alex Graves, Greg Wayne, and Ivo Danihelka. Neural turing machines. *arXiv preprint arXiv:1410.5401*, 2014.
- [GWR⁺16] Alex Graves, Greg Wayne, Malcolm Reynolds, Tim Harley, Ivo Danihelka, Agnieszka Grabska-Barwińska, Sergio Gómez Colmenarejo, Edward Grefenstette, Tiago Ramalho, John Agapiou, et al. Hybrid computing using a neural network with dynamic external memory. *Nature*, 538(7626):471, 2016.
- [HAE16] Minyoung Huh, Pulkit Agrawal, and Alexei A Efros. What makes imagenet good for transfer learning? *arXiv preprint arXiv:1608.08614*, 2016.
- [HM18] Drew A. Hudson and Christopher D. Manning. Compositional attention networks for machine reasoning. *International Conference on Learning Representations*, 2018.
- [HM19] Drew A Hudson and Christopher D Manning. Learning by abstraction: The neural state machine. *arXiv preprint arXiv:1907.03950*, 2019.
- [HRS19] Monica Haurilet, Alina Roitberg, and Rainer Stiefelhagen. It’s not about the journey; it’s about the destination: Following soft paths under question-guidance for visual reasoning. In *Proceedings of the IEEE Conference on Computer Vision and Pattern Recognition*, pages 1930–1939, 2019.

- [HS97] Sepp Hochreiter and Jürgen Schmidhuber. Long short-term memory. *Neural computation*, 9(8):1735–1780, 1997.
- [HZRS16] Kaiming He, Xiangyu Zhang, Shaoqing Ren, and Jian Sun. Deep residual learning for image recognition. In *Proceedings of the IEEE conference on computer vision and pattern recognition*, pages 770–778, 2016.
- [IS18] Vladimir Iglovikov and Alexey Shvets. Ternaunet: U-net with vgg11 encoder pre-trained on imagenet for image segmentation. *arXiv preprint arXiv:1801.05746*, 2018.
- [IYF16] Ilija Ilievski, Shuicheng Yan, and Jiashi Feng. A focused dynamic attention model for visual question answering. *arXiv preprint arXiv:1604.01485*, 2016.
- [JBM⁺18] TS Jayram, Younes Bouhadjar, Ryan L McAvoy, Tomasz Kornuta, Alexis Asseman, Kamil Rocki, and Ahmet S Ozcan. Learning to remember, forget and ignore using attention control in memory. *arXiv preprint arXiv:1809.11087*, 2018.
- [JHvdM⁺17a] Justin Johnson, Bharath Hariharan, Laurens van der Maaten, Li Fei-Fei, C Lawrence Zitnick, and Ross Girshick. Clevr: A diagnostic dataset for compositional language and elementary visual reasoning. In *Proceedings of the IEEE Conference on Computer Vision and Pattern Recognition*, pages 2901–2910, 2017.
- [JHvdM⁺17b] Justin Johnson, Bharath Hariharan, Laurens van der Maaten, Judy Hoffman, Li Fei-Fei, C Lawrence Zitnick, and Ross Girshick. Inferring and executing programs for visual reasoning. In *Proceedings of the IEEE International Conference on Computer Vision*, pages 2989–2998, 2017.
- [KGC18] Alex Kendall, Yarin Gal, and Roberto Cipolla. Multi-task learning using uncertainty to weigh losses for scene geometry and semantics. In *Proceedings of the IEEE Conference on Computer Vision and Pattern Recognition*, pages 7482–7491, 2018.
- [KMM⁺18] Tomasz Kornuta, Vincent Marois, Ryan L McAvoy, Younes Bouhadjar, Alexis Asseman, Vincent Albouy, TS Jayram, and Ahmet S Ozcan. Accelerating machine learning research with mi-prometheus. In *NeurIPS Workshop on Machine Learning Open Source Software (MLOSS)*, volume 2018, 2018.
- [KOL⁺16] Jin-Hwa Kim, Kyoung-Woon On, Woosang Lim, Jeonghee Kim, Jung-Woo Ha, and Byoung-Tak Zhang. Hadamard product for low-rank bilinear pooling. *arXiv preprint arXiv:1610.04325*, 2016.
- [KRS⁺19] Tomasz Kornuta, Deepta Rajan, Chaitanya Shivade, Alexis Asseman, and Ahmet S Ozcan. Leveraging medical visual question answering with supporting facts. *arXiv preprint arXiv:1905.12008*, 2019.
- [KSH12] Alex Krizhevsky, Ilya Sutskever, and Geoffrey E Hinton. Imagenet classification with deep convolutional neural networks. In *Advances in neural information processing systems*, pages 1097–1105, 2012.
- [KSL19] Simon Kornblith, Jonathon Shlens, and Quoc V Le. Do better imagenet models transfer better? In *Proceedings of the IEEE Conference on Computer Vision and Pattern Recognition*, pages 2661–2671, 2019.

- [KYK⁺18] Daesik Kim, YoungJoon Yoo, Jee-Soo Kim, Sangkuk Lee, and Nojun Kwak. Dynamic graph generation network: Generating relational knowledge from diagrams. In *Proceedings of the IEEE Conference on Computer Vision and Pattern Recognition*, pages 4167–4175, 2018.
- [LBH15] Yann LeCun, Yoshua Bengio, and Geoffrey Hinton. Deep Learning. *Nature*, 521(7553):436, 2015.
- [MF14] Mateusz Malinowski and Mario Fritz. A multi-world approach to question answering about real-world scenes based on uncertain input. In *Advances in neural information processing systems*, pages 1682–1690, 2014.
- [MHSJH17] Jonghwan Mun, Paul Hongsuck Seo, Ilchae Jung, and Bohyung Han. Marioqa: Answering questions by watching gameplay videos. In *Proceedings of the IEEE International Conference on Computer Vision*, pages 2867–2875, 2017.
- [MJA⁺18] Vincent Marois, TS Jayram, Vincent Albouy, Tomasz Kornuta, Younes Bouhadjar, and Ahmet S Ozcan. On transfer learning using a MAC model variant. In *NeurIPS’18 Visually-Grounded Interaction and Language (ViGIL) Workshop*, 2018.
- [MKK19] Aditya Mogadala, Marimuthu Kalimuthu, and Dietrich Klakow. Trends in integration of vision and language research: A survey of tasks, datasets, and methods. *arXiv preprint arXiv:1907.09358*, 2019.
- [MSC⁺13] Tomas Mikolov, Ilya Sutskever, Kai Chen, Greg S Corrado, and Jeff Dean. Distributed representations of words and phrases and their compositionality. In *Advances in neural information processing systems*, pages 3111–3119, 2013.
- [MTSM18] David Mascharka, Philip Tran, Ryan Soklaski, and Arjun Majumdar. Transparency by design: Closing the gap between performance and interpretability in visual reasoning. In *Proceedings of the IEEE conference on computer vision and pattern recognition*, pages 4942–4950, 2018.
- [PGC⁺17] Adam Paszke, Sam Gross, Soumith Chintala, Gregory Chanan, Edward Yang, Zachary DeVito, Zeming Lin, Alban Desmaison, Luca Antiga, and Adam Lerer. Automatic differentiation in PyTorch. *NIPS 2017 Workshop Autodiff*, 2017.
- [PNI⁺18] Matthew E Peters, Mark Neumann, Mohit Iyyer, Matt Gardner, Christopher Clark, Kenton Lee, and Luke Zettlemoyer. Deep contextualized word representations. *arXiv preprint arXiv:1802.05365*, 2018.
- [PSDV⁺18] Ethan Perez, Florian Strub, Harm De Vries, Vincent Dumoulin, and Aaron Courville. Film: Visual reasoning with a general conditioning layer. In *Thirty-Second AAAI Conference on Artificial Intelligence*, 2018.
- [PSM14] Jeffrey Pennington, Richard Socher, and Christopher Manning. Glove: Global vectors for word representation. In *Proceedings of the 2014 conference on empirical methods in natural language processing (EMNLP)*, pages 1532–1543, 2014.
- [PY09] Sinno Jialin Pan and Qiang Yang. A survey on transfer learning. *IEEE Transactions on knowledge and data engineering*, 22(10):1345–1359, 2009.

- [RDGF16] Joseph Redmon, Santosh Divvala, Ross Girshick, and Ali Farhadi. You only look once: Unified, real-time object detection. In *Proceedings of the IEEE conference on computer vision and pattern recognition*, pages 779–788, 2016.
- [Rip93] Brian D Ripley. Statistical aspects of neural networks. *Networks and chaos—statistical and probabilistic aspects*, 50:40–123, 1993.
- [SRB⁺17] Adam Santoro, David Raposo, David G Barrett, Mateusz Malinowski, Razvan Pascanu, Peter Battaglia, and Timothy Lillicrap. A simple neural network module for relational reasoning. In *Advances in neural information processing systems*, pages 4967–4976, 2017.
- [SSCH18] Xiaomeng Song, Yucheng Shi, Xin Chen, and Yahong Han. Explore multi-step reasoning in video question answering. In *2018 ACM Multimedia Conference on Multimedia Conference*, pages 239–247. ACM, 2018.
- [SZ14] Karen Simonyan and Andrew Zisserman. Very deep convolutional networks for large-scale image recognition. *arXiv preprint arXiv:1409.1556*, 2014.
- [TLvdH17] Damien Teney, Lingqiao Liu, and Anton van den Hengel. Graph-structured representations for visual question answering. In *Proceedings of the IEEE Conference on Computer Vision and Pattern Recognition*, pages 1–9, 2017.
- [VSP⁺17] Ashish Vaswani, Noam Shazeer, Niki Parmar, Jakob Uszkoreit, Llion Jones, Aidan N Gomez, Łukasz Kaiser, and Illia Polosukhin. Attention is all you need. In *Advances in Neural Information Processing Systems*, pages 5998–6008, 2017.
- [WCB14] Jason Weston, Sumit Chopra, and Antoine Bordes. Memory networks. *arXiv preprint arXiv:1410.3916*, 2014.
- [WDS⁺19] Thomas Wolf, Lysandre Debut, Victor Sanh, Julien Chaumond, Clement Delangue, Anthony Moi, Pierric Cistac, Tim Rault, Rémi Louf, Morgan Funtowicz, et al. Transformers: State-of-the-art natural language processing. *arXiv preprint arXiv:1910.03771*, 2019.
- [WKW16] Karl Weiss, Taghi M Khoshgoftaar, and DingDing Wang. A survey of transfer learning. *Journal of Big data*, 3(1):9, 2016.
- [WM96] Brad Warner and Manavendra Misra. Understanding neural networks as statistical tools. *The american statistician*, 50(4):284–293, 1996.
- [XMS16] Caiming Xiong, Stephen Merity, and Richard Socher. Dynamic memory networks for visual and textual question answering. In *International conference on machine learning*, pages 2397–2406, 2016.
- [XZX⁺17] Dejing Xu, Zhou Zhao, Jun Xiao, Fei Wu, Hanwang Zhang, Xiangnan He, and Yueting Zhuang. Video question answering via gradually refined attention over appearance and motion. In *Proceedings of the 25th ACM international conference on Multimedia*, pages 1645–1653. ACM, 2017.
- [YGW⁺18] Guangyu Robert Yang, Igor Ganichev, Xiao-Jing Wang, Jonathon Shlens, and David Sussillo. A dataset and architecture for visual reasoning with a working memory. In *European Conference on Computer Vision*, pages 729–745. Springer, 2018.

- [YHG⁺16] Zichao Yang, Xiaodong He, Jianfeng Gao, Li Deng, and Alex Smola. Stacked attention networks for image question answering. In *Proceedings of the IEEE conference on computer vision and pattern recognition*, pages 21–29, 2016.
- [YKCK17] Youngjae Yu, Hyungjin Ko, Jongwook Choi, and Gunhee Kim. End-to-end concept word detection for video captioning, retrieval, and question answering. In *Proceedings of the IEEE Conference on Computer Vision and Pattern Recognition*, pages 3165–3173, 2017.
- [YTXW19] Chengxiang Yin, Jian Tang, Zhiyuan Xu, and Yanzhi Wang. Memory augmented deep recurrent neural network for video question answering. *IEEE transactions on neural networks and learning systems*, 2019.
- [ZSS⁺18] Amir R Zamir, Alexander Sax, William Shen, Leonidas J Guibas, Jitendra Malik, and Silvio Savarese. Taskonomy: Disentangling task transfer learning. In *Proceedings of the IEEE Conference on Computer Vision and Pattern Recognition*, pages 3712–3722, 2018.
- [ZTS⁺15] Bolei Zhou, Yuandong Tian, Sainbayar Sukhbaatar, Arthur Szlam, and Rob Fergus. Simple baseline for visual question answering. *arXiv preprint arXiv:1512.02167*, 2015.

7 Datasets: COG & CLEVR-CoGenT

Variant	number of frames	maximum memory duration	maximum number of distractors	size of training set	size of validation set	size of test set
Canonical	4	3	1	10000320	500016	500016
Hard	8	7	10	10000320	500016	500016

Table 3: Details of the Canonical and Hard variants of the COG dataset.

Dataset	Cubes	Cylinders	Spheres
CoGenT-A	Gray / Blue / Brown / Yellow	Red / Green / Purple / Cyan	Any color
CoGenT-B	Red / Green / Purple / Cyan	Gray / Blue / Brown / Yellow	Any color

Table 4: Colors & shapes combinations present in CoGenT-A & -B datasets.

The CoGenT dataset [JHvdM⁺17a] contains:

- Training set of 70,000 images and 699,960 questions in Condition A,
- Validation set of 15,000 images and 149,991 questions in Condition A,
- Test set of 15,000 images and 149,980 questions in Condition A (without answers),
- Validation set of 15,000 images and 150,000 questions in Condition B,
- Test set of 15,000 images and 149,992 questions in Condition B (without answers),
- Scene graphs and functional programs for all training/validation images/questions.

8 Complete COG results

Table 5: COG test set accuracies for SAMNet & COG models. Below ‘paper’ denotes results from [YGW⁺18] while ‘code’ denotes results of our experiments using their implementation [Gan18].

Model	SAMNet				COG Model			
	canonical	canonical	canonical	hard	paper	ours	ours	paper
					canonical	canonical	canonical	hard
					-	-	hard	-
Trained on	canonical	hard	hard	hard	canonical	hard	hard	hard
Fine tuned on	-	-	hard	-	-	-	hard	-
Tested on	canonical	hard	hard	hard	canonical	hard	hard	hard
Overall accuracy	98.0	91.6	96.5	96.1	97.6	65.9	78.1	80.1
AndCompareColor	93.5	82.7	89.2	80.6	81.9	57.1	60.7	51.4
AndCompareShape	93.2	83.7	89.7	80.1	80.0	53.1	50.3	50.7
AndSimpleCompareColor	99.2	85.3	97.6	99.4	99.7	53.4	77.1	78.2
AndSimpleCompareShape	99.2	85.8	97.6	99.2	100.0	56.7	79.3	77.9
CompareColor	98.1	89.3	95.9	99.7	99.2	56.1	67.9	50.1
CompareShape	98.0	89.7	95.9	99.2	99.4	66.8	65.4	50.5
Exist	100.0	99.7	99.8	99.8	100.0	63.5	96.1	99.3
ExistColor	100.0	99.6	99.9	99.9	99.0	70.9	99	89.8
ExistColorOf	99.9	95.5	99.7	99.8	99.7	51.5	76.1	73.1
ExistColorSpace	94.1	88.8	91.0	90.8	98.9	72.8	77.3	89.2
ExistLastColorSameShape	99.5	99.4	99.4	98.0	100.0	65.0	62.5	50.4
ExistLastObjectSameObject	97.3	97.5	97.7	97.5	98.0	77.5	61.7	60.2
ExistLastShapeSameColor	98.2	98.5	98.8	97.5	100.0	87.8	60.4	50.3
ExistShape	100.0	99.5	100.0	100.0	100.0	77.1	98.2	92.5
ExistShapeOf	99.4	95.9	99.2	99.2	100.0	52.7	74.7	72.70
ExistShapeSpace	93.4	87.5	91.1	90.5	97.7	70	89.8	89.80
ExistSpace	95.3	89.7	93.2	93.3	98.9	71.1	88.1	92.8
GetColor	100.0	95.8	99.9	100.0	100.0	71.4	83.1	97.9
GetColorSpace	98.0	90.0	95.0	95.4	98.2	71.8	73.	92.3
GetShape	100.0	97.3	99.9	99.9	100.0	83.5	89.2	97.1
GetShapeSpace	97.5	89.4	93.9	94.3	98.1	78.7	77.3	90.3
SimpleCompareShape	99.9	91.4	99.7	99.9	100.0	67.7	96.7	99.3
SimpleCompareColor	100.0	91.6	99.80	99.9	100.0	64.2	90.4	99.3

9 Complete CLEVR-CoGenT results

Table 6: Complete set of results for SAMNet on CLEVR-CoGenT.

Experiments	Test Accuracy (%)					
	on valA – 150,000 samples					
	Overall	Exist	Count	CompareInteger	CompareAttribute	QueryAttribute
Exist only	26.07	<i>74.20</i>	0.0	59.79	59.15	0.0
Count only	14.89	0.0	<i>62.78</i>	0.0	0.0	0.0
CompareInteger only	23.44	48.15	0.0	<i>77.98</i>	54.08	0.0
CompareAttribute only	23.50	51.93	0.0	59.06	<i>61.73</i>	0.0
QueryAttribute only	34.64	0.0	0.0	0.0	0.0	<i>97.08</i>
All tasks	95.32	98.4	86.75	96.0	98.65	98.02
All tasks but Exist	90.33	<i>60.42</i>	86.12	96.18	98.52	98.60
All tasks but Count	74.59	97.51	<i>0.0</i>	94.37	98.42	98.47
All tasks but CompareInteger	91.53	98.22	86.09	<i>56.35</i>	98.78	98.40
All tasks but CompareAttribute	81.92	98.32	86.36	95.86	<i>23.18</i>	98.44
All tasks but QueryAttribute	42.17	76.79	54.64	79.87	64.13	<i>0.0</i>
<i>Trained on all tasks – Finetune on t</i>						
Exist	94.16	<i>98.04</i>	82.96	95.02	98.12	97.97
Count	95.10	96.46	<i>88.28</i>	94.78	97.01	98.26
CompareInteger	95.31	98.39	86.56	<i>96.07</i>	98.70	98.09
CompareAttribute	95.31	98.40	86.78	96.00	<i>98.66</i>	98.04
QueryAttribute	93.49	97.45	82.09	92.23	97.85	<i>97.76</i>